**Biogeosciences**
Open Access
Discussions

# Disentangling the response of forest and grassland energy exchange to heatwaves under idealized land–atmosphere coupling

**C. C. van Heerwaarden**[1] **and A. J. Teuling**[2]

[1]Max Planck Institute for Meteorology, Hamburg, Germany
[2]Hydrology and Quantitative Water Management Group, Wageningen University, Wageningen, the Netherlands

Correspondence to: C. C. van Heerwaarden (chiel.vanheerwaarden@mpimet.mpg.de)

---

Discussion Paper | Discussion Paper | Discussion Paper | Discussion Paper

**BGD**

11, 5969–5995, 2014

**Forest and grassland energy exchange**

C. C. van Heerwaarden and A. J. Teuling

Title Page

| Abstract | Introduction |
| Conclusions | References |
| Tables | Figures |

|◄ | ►|

◄ | ►

Back | Close

Full Screen / Esc

Printer-friendly Version

Interactive Discussion

C. C. van Heerwaarden and A. J. Teuling

## Abstract

This study investigates the difference in land–atmosphere interactions between grassland and forest during typical heat wave conditions in order to understand the controversial results of Teuling et al. (2010) (T10, hereafter), who have found the systematic occurrence of higher sensible heat fluxes over forest than over grassland during heat wave conditions. With a simple, but accurate coupled land–atmosphere model, we are able to reproduce the findings of T10 for both normal summer and heat wave conditions, and to carefully explore the sensitivity of the coupled land–atmosphere system to changes in incoming radiation and early-morning temperature. Our results emphasize the importance of fast processes during the onset of heat waves, since we are able to explain the results of T10 without having to take into account changes in soil moisture.

In order to disentangle the contribution of differences in several static and dynamic properties between forest and grassland, we have performed an experiment in which new land use types are created that are equal to grassland, but with one of its properties replaced by that of forest. From these, we conclude that the closure of stomata in the presence of dry air is by far the most important process in creating the different behavior of grassland and forest during the onset of a heat wave. However, we conclude that for a full explanation of the results of T10 also the other properties (albedo, roughness and the ratio of minimum stomatal resistance to leaf-area index) play an important, but indirect role; their influences mainly consist of strengthening the feedback that leads to the closure of the stomata by providing more energy that can be converted into sensible heat. The model experiment also confirms that, in line with the larger sensible heat flux, higher atmospheric temperatures occur over forest.

## 1 Introduction

There are strong indications that the intensity and frequency of midlatitude heat waves has increased over the last decades, but the degree to which this can be attributed

to human influence on the climate is uncertain (IPCC, 2013). Since local land surface conditions can strongly impact temperatures during heatwaves (Miralles et al., 2012), any changes in land surface conditions, for instance through land use change, have the potential to impact temperature extremes. Probably the most striking example of

5　land-use change in the world is deforestation; in many parts of the world forests have been converted into grassland over the last centuries (e.g., Christidis et al., 2013). Despite the fact that deforestation has been recognized as an important driver of local climate change (Davin and de Noblet-Ducoudré, 2010; Bonan, 2008), its effect on heat waves is still poorly understood; Until now it is unclear whether forests reach higher

10　or lower temperatures than grassland during warm summer conditions or heat waves (Zaitchik et al., 2006; Teuling et al., 2010; Anderson et al., 2010). One of the major open questions is how and to which extent land-use affects temperature extremes during heat waves, which is shown to depend strongly on feedbacks between the land surface and the atmospheric boundary layer (Stap et al., 2014).

15　　The recent study of Teuling et al. (2010) (T10, hereafter) showed that during the early stages of a heat wave the sensible heat fluxes above forests can far exceed those over grassland, despite the common belief that forests with their deeper root systems would maintain higher evapotranspiration rates and thus dampen the strength of heat waves (Bonan, 2008). To illustrate this, Fig. 1 shows the composite relationship between mid-

20　day temperature and the preceding midday (09:00–12:00 UTC) sensible heat flux over all European forest and grassland FLUXNET sites with long-term observations taken from T10. We can induce from this figure that forest amplifies its near-surface temperature by increasing its sensible heat flux under high temperatures, whereas grassland maintains a more constant flux. This, however does not immediately imply that the

25　highest temperatures occur over forest, as the temperature increase due to the extra sensible heat flux is (partly) offset by increased mixing above the canopy due to the higher roughness of forest.

　　In this paper, we aim at improving our understanding of the mechanisms that drive the behavior reported by T10 and Fig. 1 by means of a modeling experiment of the

Title Page

Abstract　　Introduction

Conclusions　　References

Tables　　Figures

⏮　　⏭

◀　　▶

Back　　Close

Full Screen / Esc

Printer-friendly Version

Interactive Discussion

coupled land surface-atmospheric boundary layer system. In order to provide a theoretical framework for our analysis, we start this study by explaining the differences in feedback loops that regulate the atmospheric control on evapotranspiration between forest and grassland (Sect. 2).

5    For our modeling experiment we use a coupled model that consists of a bulk schematization for the atmospheric boundary layer, a force-restore land surface scheme, and a basic radiation scheme (van Heerwaarden et al., 2010a, b; Vilà-Guerau de Arellano et al., 2012). The essence of our experiment is that we model a typical day in order to show that the modeling of fast processes is sufficient to explain the first order re-
10  sponse of the coupled land–atmosphere system to heat wave conditions. The relevant fast processes in this study are the atmospheric turbulence, the opening and closure of the stomata of the vegetation, and the response time of the surface temperature, which all have time scales less than tens of minutes. The model and the experiments are described in Sect. 3. Our modeling experiment consists of three phases. First, we
15  evaluate our model against observations reported in T10 for normal summer and heat wave conditions (Sect. 4.1). Then, we perform a sensitivity study on the external forcings and show how the surface energy balance, atmospheric temperature and humidity and the boundary layer height respond to changes in the incoming radiation and the large scale temperature forcing (Sect. 4.2). To conclude, we analyze the differences be-
20  tween forest and grassland in detail, by comparing the relative importance of properties of the land surface that are different between forest and grass: the albedo, the vapor pressure deficit response, the ratio of the leaf-area-index to the minimum resistance and the roughness (Sect. 4.3).

In our model, we represent forest in the same way as in the majority of the numerical
25  weather prediction and climate models (e.g. Noilhan and Mahfouf, 1996; Ek et al., 2003), in order to keep the same level of complexity among all model components. We are aware of the simplified treatment of the forest, but the exponential relationship between vapor pressure deficit (VPD) and stomatal resistance, which forms the core

**Forest and grassland energy exchange**

C. C. van Heerwaarden and A. J. Teuling

Full Screen / Esc

Printer-friendly Version

Interactive Discussion

of our parametrization (see Sect. 3), has been found in many experiments (Oren et al., 1999).

## 2 Land-atmosphere coupling over grassland and forest

The atmospheric control on evapotranspiration works on short time scales, because the
5  atmospheric boundary layer is turbulent. Therefore, during daytime heat and moisture
are efficiently taken away from the surface and mixed throughout this layer on time
scales on the order of tens of minutes. Over grasslands this leads to a system with three
dominant negative feedback loops that are discussed in detail in van Heerwaarden
et al. (2009) and shortly summarized here (see Fig. 2).
10    First, there is the heating feedback, where heating of the atmosphere, either direct
or indirect through entrainment by boundary layer growth, increases the capacity for
water and therefore the potential evaporation. Second, there is the drying feedback.
Throughout the day the turbulent atmospheric boundary layer grows, and therefore
brings in dry air from the free atmosphere above the atmospheric boundary layer. The
15  drying of the air reduces the degree to which the atmospheric capacity for water has
been met and therefore also enhances the potential evaporation. Third, the moistening
feedback takes into account that the evapotranspiration reduces when the atmosphere
fills up with evaporated water. These three feedback loops direct the system towards
a state defined as equilibrium evaporation (Raupach, 2000, 2001; van Heerwaarden
20  et al., 2009). For grasslands we conclude that on short time scales, changes in the
actual evapotranspiration rate are driven by changes in the temperature and humidity
in the atmospheric boundary layer and therefore in the potential evaporation rate.
    The feedback loops in the system are more complex over forest, where changes in
the actual evapotranspiration rate are no longer only driven by changes in the potential
25  evaporation rate. Instead, an additional connection is added that includes the dynamics
of the vegetation itself into all feedback loops. From the temperature and moisture it is
possible to derive the VPD, which is a measure of the dryness of the air. Tree leaf

Full Screen / Esc

Printer-friendly Version

Interactive Discussion

C. C. van Heerwaarden and A. J. Teuling

Full Screen / Esc

Printer-friendly Version

Interactive Discussion

stomata are known to react strongly to increasing dryness of the air by letting the trees close their stomata. The stomatal resistance, to which the evapotranspiration rate is inversely proportional, increases thus under a larger VPD (Oren et al., 1999). This has a dramatic effect on the behavior of the system; over grassland each increase in the VPD leads to an increase in evapotranspiration, whereas over forest there is a competition between the enhancement of the potential evaporation and the increase in the stomatal resistance. As soon as the latter effect becomes stronger, all feedback loops change from negative to positive: more heating and drying leads to a higher VPD, a larger stomatal resistance and less evapotranspiration, which in turn leads to more heating and drying. We show in Sect. 4.2 that the shift of the system from one that evolves towards equilibrium evaporation to one that evolves towards very low evapotranspiration rates leaves a distinct signal in the results.

## 3  Methods

### 3.1  Coupled land–atmosphere model

This study uses a simple, but accurate model of the coupled land–atmosphere system that has been explained in detail in van Heerwaarden et al. (2010a). The atmospheric part of the model is a bulk model for the convective boundary layer (Tennekes, 1973). Furthermore, it has a simplified radiation parametrization that provides the incoming short and long wave radiation to the system. The surface energy balance at the land surface is solved using the Penman–Monteith equation (Monteith, 1965) and the heat and moisture transport in the soil is described using a force-restore model (Noilhan and Mahfouf, 1996).

Since this study is about the differences between grassland and forest, we focus here only on the properties that control these differences and how these are implemented in the model. The albedo $\alpha$ is used in the calculation of the net short wave radiation $S_{net}$

following:

$$S_{net} = (1 - cc)(1 - \alpha)S_{in}, \tag{1}$$

where $S_{in}$ is the incoming shortwave radiation and cc is the cloud cover. The albedo influences therefore the amount of net radiation available for the sensible, latent and soil heat flux. Note that we only take the shortwave effect of clouds into account.

The roughness lengths $z_{0m}$ and $z_{0h}$ enter in the calculation of the drag coefficient (Paulson, 1970), to which the aerodynamic resistance $r_a$, is inversely proportional. The aerodynamic resistance is included in the evapotranspiration calculation:

$$LE \propto \frac{1}{r_a + r_s}, \tag{2}$$

where LE is the latent heat flux or evapotranspiration and $r_s$ the stomatal resistance.

Two main properties determine the calculation of the stomatal resistance $r_s$: the ratio of the minimal stomatal resistance to the leaf-area index, and the response of the stomata to environmental conditions. The former because it determines to which extent potential evaporation (at $r_s = 0\,\mathrm{s\,m^{-1}}$) can be met under unstressed conditions (see Eq. 2) and the latter as it takes into account (amongst other things) the previously discussed strong response of tree leaf stomata to vapor pressure deficit. The $r_s$ is calculated following Jarvis (1976):

$$r_s = \frac{r_{s,\,min}}{LAI} f_1(S_{in}) f_2(w) f_3(VPD) f_4(T) \tag{3}$$

where $f_n$ are correction functions for a certain variable, $w$ is the soil moisture and $T$ is the atmospheric temperature at the vegetation level. The response function $f_3$ to vapor pressure deficit VPD can be described by:

$$f_3 = e^{g_D VPD} \tag{4}$$

where $g_D$ an empirical constant that describes the strength of the response of the vegetation to the vapor pressure deficit. The other correction functions are discussed in van Heerwaarden et al. (2010a).

## 3.2 Modeling experiment

In our modeling experiment, we focus on the daytime conditions and the response of vegetation to heat waves on the time scales of turbulence. This means that we restrict our model simulations to a single day, as this is long enough to draw conclusions on the response of fast processes. The atmospheric temperature, humidity and wind profiles that we provide to the model are representative for western European summer conditions. An overview of the specific parameters for grassland and forest is shown in Table 1 and a detailed list of all parameters is given in Table A1 in the Appendix. A similar approach has been followed in van Heerwaarden et al. (2010b), but then for the Great Plains in the USA.

We tune the cloud cover and the soil moisture of the model such that it produces values of the incoming radiation and partitioning between sensible and latent heat fluxes that are consistent with observations in T10. We stress here that our aim is not to exactly reproduce the data, but rather to demonstrate the behavior of the system and to make an assessment of the most important links in the coupled system. In Fig. 4 and onward, we look at the sensitivity of the system to any change in initial temperature and incoming radiation.

After establishing the mean state that represents T10's data, we continue by performing a sensitivity study on the incoming radiation by varying the cloud cover and the early-morning temperature. In order to do a proper experiment on the early-morning temperature, we shift the entire atmospheric potential temperature profile and the near surface soil temperature towards new values, such that the vertical gradients are maintained. Based on this new profile, we perturb the specific humidity, such that we maintain the same initial relative humidity in all our experiments, to allow for a fair comparison. Since the model is fast, we can explore a large number of combinations. Within these simulation results, we locate the heat wave conditions that match the short wave radiation anomaly and temperature anomaly that T10 has reported.

Title Page

Abstract | Introduction

Conclusions | References

Tables | Figures

◀ | ▶

◀ | ▶

Back | Close

Full Screen / Esc

Printer-friendly Version

Interactive Discussion

Then, in order to understand better the importance of the individual properties that distinguishes forest from grassland in our model (albedo, roughness length, stomatal response to VPD and ratio of the minimal resistance to the leaf area index), we redo our sensitivity study again, but with newly created land use types that resemble grassland with one of the four properties of forest attached to it. With this approach we can estimate the relative importance of each property and the degree to which the different properties weaken or strengthen each other.

## 4 Results

### 4.1 Reproduction of the measurements

The model setup described in Sect. 3 is able to reproduce the most important characteristics of the measurements. Figure 3 shows the surface energy balance under average forcings and under typical heat wave condions and can directly be compared with T10's Fig. 1b and 1d. Since we have tuned the radiation and the soil moisture contents to reproduce T10's mean state in the best possible way, the match is not surprising. The heat wave state, which has been achieved by only perturbing the incoming radiation and the early morning temperature of the mean state, is reproduced well by the model; all modeled anomalies follow the data of T10 and especially the enhanced sensible heat flux over forest of approximately $125\,\mathrm{W\,m^{-2}}$ ($121\,\mathrm{W\,m^{-2}}$ in T10) is reproduced well. This finding implies that the model, and therefore parametrizations in existing numerical weather prediction and climate models, are able to reproduce the response of forests to perturbations in the incoming radiation and temperature.

### 4.2 The sensitivity of grassland and forest to incoming short wave radiation and temperature

Figures 4 and 5 show the results of the entire sensitivity study of which the day that is contained in Fig. 3a has been perturbed. Figure 4 illustrates the sensitivity of the net

radiation, the evapotranspiration and the sensible heat flux to the incoming radiation and the early morning temperature for both forest and grass.

The surface energy balance and the atmospheric properties of grassland change monotonically under changes in the radiation and the early-morning temperature, whereas those of forest displays more complex behavior. As we already have hypothesized in Sect. 2, grassland mostly responds to the changes in the potential evaporation, an increase in temperature or radiation automatically results in an increase in evapotranspiration, with a uniform sensitivity over the majority of the parameter range. The net radiation is logically mostly sensitive to changes in the incoming short wave radiation. Nonetheless, a slight reduction in net radiation is observed with increasing temperature ($5\,\mathrm{W\,m^{-2}}$ over the entire temperature range), which is related to the increase in surface temperature and the consequent increase in the outgoing long wave radiation.

Forest has a maximum in evapotranspiration and a minimum in the sensible heat flux for given high values of incoming radiation (located at an early morning temperature of $297\,\mathrm{K}$ for an incoming radiation of $500\,\mathrm{W\,m^{-2}}$, until a temperature of $291\,\mathrm{K}$ for $750\,\mathrm{W\,m^{-2}}$). At low early-morning temperatures, the increase in potential evaporation related to the higher temperatures is the dominant effect. However, the decrease in actual evapotranspiration due to the higher stomatal resistance is the strongest effects at higher temperatures, resulting in a reduction of evapotranspiration with an increase in early morning temperature. Over forest, the change in sensible heat flux with early morning temperature is non-monotonic as well.

In order to explain the observations shown in Fig. 1, we have marked (black dotted lines, indicating the 93 to $105\,\mathrm{W\,m^{-2}}$ interval) the combinations of incoming short wave radiation and initial temperature that give a constant sensible heat flux over grassland in the same range as that in Fig. 1. Within this range, the sensible heat flux of forest increases in the direction of heatwave conditions (high temperature and incoming radiation) from approximately $115\,\mathrm{W\,m^{-2}}$ to values more than $200\,\mathrm{W\,m^{-2}}$ while moving to higher values for incoming radiation and initial temperature. This behavior matches

very well with what is found in Fig. 1 and reconfirms the suggested mechanisms in Sect. 2.

The differences in surface energy balance between grassland and forest are reflected in the atmospheric boundary layer characteristics (Fig. 5). The shaded region shows the maximum two-meter temperature that is achieved during the day. Under conditions of low early-morning temperatures and a small amount of incoming radiation, which are found in the bottom left of the plots, the maximum two-meter temperature is comparable for grassland and forest ($\sim 293\,\mathrm{K}$ for an early morning temperature of $283\,\mathrm{K}$ and an incoming shortwave radiation of $500\,\mathrm{W\,m^{-2}}$). While we move towards the top right in the plots, thus to higher early-morning temperatures and more incoming shortwave radiation, the maximum temperature over forest increases considerably faster over forest ($313\,\mathrm{K}$) than over grassland ($308\,\mathrm{K}$). In Fig. 4, we have seen that this is due to an increase in the sensible heat fluxes over forest that is not found over grassland.

The changes in the VPD show the increased drying of the atmosphere over the forest (solid blue lines, Fig. 5). While grassland has a range from 12 to 26 hPa over the entire parameter space, the VPD over the forest increases from 13.5 to 38 hPa, which is a much wider range than that over grassland.

The occurrence of a maximum evapotranspiration rate with increasing temperature is reflected in the achieved atmospheric boundary layer heights (dashed red lines, Fig. 5). Grassland shows again a monotonic behavior; the boundary layer height increases with increasing incoming short wave radiation due to the extra available energy, whereas the boundary layer height decreases under rising early-morning temperatures, due to the shift of energy from sensible to latent heating.

The achieved boundary layer heights over forest show a curved line that displays an minimum with respect to early-morning temperature close to values of $296\,\mathrm{K}$ for high values of incoming shortwave radiation. This minimum is directly related to the maximum evapotranspiration that was found in Fig. 4 and the result of the VPD-related

**Forest and grassland energy exchange**

C. C. van Heerwaarden and A. J. Teuling

Title Page

Abstract | Introduction

Conclusions | References

Tables | Figures

|◄ | ►|

◄ | ►

Back | Close

Full Screen / Esc

Printer-friendly Version

Interactive Discussion

feedback mechanism that is also responsible the minimum in sensible heat flux found over forest.

## 4.3 Unraveling the feedback mechanisms

In the previous section we have shown that we are able to reproduce the measurements of T10 with our model. The aim of the current section is to find the relative importance of each of the differences in properties between grassland and forest in creating the big difference between the two land use types that was found in the measurements of T10. With our model we compare the response of the coupled system to perturbations in incoming radiation and temperature for a set of land use types. This set contains grassland and forest itself, but also types that have the properties of grassland and one of the properties of forest, such that we can assess the influence of each forest property separately.

Figure 6 shows the difference between grassland and forest, the influence of the four properties separately and the importance of the interaction between the feedbacks. Figure 6a shows the difference in evapotranspiration, maximum temperature and net radiation that is the result of subtracting the values of grassland from those of forest, which are shown in Figs. 4 and 5.

The first property that we take into consideration is the albedo. The most importance change to the system if the albedo of forest is attributed to the grassland is the increase in net radiation for forest, because it has a lower albedo than grassland. The difference increases from 36 to 56 W m$^{-2}$ over the range of shortwave radiation on the horizontal axis, where forest, with its lower albedo, converts more of the extra incoming short wave radiation to net radiation. The evapotranspiration ($\sim 25$ W m$^{-2}$) and the maximum temperature ($\sim 0.8$ K) show an increase over the entire parameter range, but have a low sensitivity to changes in the radiation or early-morning temperature.

The second property is roughness. If we increase the roughness of the grassland to that of forest, then the evapotranspiration, maximum temperature and net radiation are affected. In all three variables, the strongest changes occur under a low early morn-

C. C. van Heerwaarden and A. J. Teuling

ing temperature and a high incoming shortwave radiation, because here the sensible heat flux is the highest. We suggest that the changes are the effect of a sequence of events that starts with an increased mixing near the surface, due to the higher roughness. Subsequently, the near-surface temperature resembles more that of its overlying

5 atmosphere and drops. Then, the outgoing long wave radiation decreases, resulting in an increase of the available energy for the sensible and latent heat flux. This results in a slightly increased evapotranspiration and sensible heat flux, with an eventual rise in maximum temperature despite the stronger mixing. This interpretation is applicable to the entire range of incoming radiation and early-morning temperatures. All in all, the

10 sensitivity of the system to roughness is relatively low compared to the other properties, which is in line with the previous findings of Hill et al. (2008).

The third property that we study is the stomatal response to vapor pressure deficit. We already identified the closure of stomata as a response to dry air as a potential mechanism to strongly reduce the evapotranspiration before, in Sect. 2. Figure 6 de-

15 livers a quantitative confirmation of this hypothesis. Without major modifications to the net radiation, the inclusion of this forest property to grassland results in a large drop in evapotranspiration (up to $100\,\mathrm{W\,m^{-2}}$) and a consequent increase in the maximum temperature (more than $2.6\,\mathrm{K}$) through an enhanced sensible heat flux over the entire parameter space. The strength of the drying of the atmosphere is reflected in the larger

20 VPD over forest than grassland (more than $15\,\mathrm{hPa}$).

The fourth and last property included in the study is the ratio of minimum stomatal resistance to the leaf-area index (see 3), which is a measure of the maximal potential of the plants to transpire under unstressed soil moisture conditions. Since forest has a lower value, it has a lower stomatal resistance under unstressed conditions and there-

25 fore significantly higher evapotranspiration rates (30 to $50\,\mathrm{W\,m^{-2}}$ more than grassland). Hill et al. (2008) already pointed out the importance of the leaf area index. The higher evapotranspiration rate results in significantly lower maximum temperatures over forest (more than $1.2\,\mathrm{K}$ less than grassland). The net radiation is fairly insensitive to this parameter.

C. C. van Heerwaarden and A. J. Teuling

In order to estimate to which extent the properties counteract or strengthen the effect of the other properties, we have subtracted the four individual effects from the total difference, so that a residual is acquired. We find that the reduction of evapotranspiration under increasing temperature and radiation can be more than $50\,\mathrm{W\,m^{-2}}$ larger than the sum of the four individual components. We hypothesize that the increased reduction is related to strong interactions between the effects of albedo and that of the VPD-response. Where the extra energy provided by the lower albedo is added to the evapotranspiration in Fig. 6c, this extra energy ends up in the heating in the residual. Here, the system has entered the positive feedback loop (Fig. 2), where additional energy leads to an enhanced drying and heating. The additional net radiation of approximately $50\,\mathrm{W\,m^{-2}}$, results in an enhanced reduction in evapotranspiration of the same amount of energy and an additional increase in the maximum temperature of $1\,\mathrm{K}$, almost 25 % of the total difference. The slight increase in net radiation, is most likely related to the interplay between the properties related to the VPD-response and the roughness. In this case, the increase in roughness counteracts the highly enhanced surface temperature that is the effect of the VPD-response. Therefore, there is a slight reduction in the outgoing long wave radiation and a corresponding small increase in the net radiation.

## 5 Conclusions

We have studied the differences in land–atmosphere coupling between grassland and forest during the onset of heat waves by means of a modeling experiment in which a typical summer day for Western European conditions has been analyzed under normal and under heat wave conditions. With a simple, but accurate conceptual model that contains the essential processes in the coupled land–atmosphere system (van Heerwaarden et al., 2010a), we are able to reproduce the observations of Teuling et al. (2010) (T10) who showed higher temperatures over forest than over grassland during the early stages of heat waves.

C. C. van Heerwaarden and A. J. Teuling

In addition to reproducing the data of T10, we have done sensitivity studies on the response of forest and grassland to perturbations of the early-morning temperature and radiation in order to mimic the forcings that correspond to heat waves. From this analysis we have learned that both grassland and forest display a monotonically in-
⁵ creasing evapotranspiration and sensible heat flux under increasing incoming short-wave radiation, because the potential evaporation increases. The reaction to increases in early-morning temperature is more complex. Although grassland shows monotonic increases in evapotranspiration and monotonic decreases in sensible heat flux and atmospheric boundary layer height under increasing early-morning temperatures, for-
¹⁰ est displays more complex behavior; beyond a critical threshold, the effects of vapor pressure deficit (VPD) on stomatal closure are stronger than the effects on the potential evaporation. Therefore, the evapotranspiration no longer increases but decreases with increasing temperature, resulting in an increasing sensible heat flux, maximum temperature and atmospheric boundary layer height.

¹⁵ Furthermore, we have repeated the sensitivity study not only for forest and grass, but also for a series of artificial land use types that are grassland with one of its properties replaced by the corresponding property of forest. Here, it was found that strong temperature increase over forest is primarily driven by the feedback mechanism that leads to an increasingly fast shutdown of evapotranspiration (Fig. 6), related to the stomatal
²⁰ closure of the leafs of trees under high values of VPD. While this finding is not a surprise, our results show that the other property differences are essential in explaining the results of T10. Mostly the lower albedo of forest plays a crucial role; Without the stomatal response to VPD the lower albedo mostly enhances the evapotranspiration by providing more energy, whereas all the extra energy is converted into sensible heat
²⁵ when the stomatal response to VPD is active.

To conclude, our results show that the high temperatures over forest compared to grassland that T10 found are mostly driven by fast processes in the atmosphere and vegetation. The good news is that the simple parametrizations that are used in our model and in most of the numerical weather prediction and climate models are able to

Title Page

Abstract | Introduction

Conclusions | References

Tables | Figures

|◀ | ▶|

◀ | ▶

Back | Close

Full Screen / Esc

Printer-friendly Version

Interactive Discussion

reproduce the heat wave response. Nonetheless, the large magnitude of the temperatures increases over forest are a complex interplay of land-surface and atmospheric boundary layer processes. We expect that as soon as the evapotranspiration fluxes start depleting the soil moisture reservoirs, the evolution of the soil moisture takes over
5   as the most crucial aspect of the system.

A logical extension of this study of idealized land-atmosphere coupling is an investigation of the exact role of land-surface heterogeneity. In our study, we have assumed that the surface and the atmosphere are in equilibrium with each other, which requires areas of uniform land use with a radius of at least tens of kilometers (Mahrt, 2000).
10  Many of the Western-European forests are smaller than this, and therefore, the air over forests partly resembles that of grasslands. The relatively moist air coming from the strongly evaporating grassland could largely suppress the effects of the VPD-related feedback (Fig. 2), making the high roughness of forest relatively more important. This could explain why several studies have reported lower surface temperatures in forests
15  under heat wave conditions.

## Appendix A

## Model parameters

Table A1 contains an overview of all chosen parameters for our model setup. We have chosen 50° N as the representative latitude for central Western Europe, the region that
20  T10 studies. Our simulations make use of idealized atmospheric profiles that match the climatology. We maintain the early morning relative humidity of our simulations, such that the specific humidity profile changes with the temperature. Our soil parameters describe a standard loamy soil.

**Forest and grassland energy exchange**

C. C. van Heerwaarden and A. J. Teuling

Title Page

Abstract | Introduction

Conclusions | References

Tables | Figures

|◄ | ►|

◄ | ►

Back | Close

Full Screen / Esc

Printer-friendly Version

Interactive Discussion

## References

Anderson, R. G., Canadell, J. G., Randerson, J. T., Jackson, R. B., Hungate, B. A., Baldocchi, D. D., Ban-Weiss, G. A., Bonan, G. B., Caldeira, K., Cao, L., Diffenbaugh, N. S., Gurney, K. R., Kueppers, L. M., Law, B. E., Luyssaert, S., and O'Halloran, T. L.: Biophysical considerations in forestry for climate protection, Front. Ecol. Environ., 9, 174–182, doi:10.1890/090179, 2010. 5971

Bonan, G. B.: Forests and climate change: forcings, feedbacks, and the climate benefits of forest, Science, 320, 1444–1449, doi:10.1126/science.1155121, 2008. 5971

Christidis, N., Stott, P. A., Hegerl, G. C., and Betts, R. A.: The role of land use change in the recent warming of daily extreme temperatures, Geophys. Res. Lett., 40, 589–594, doi:10.1002/grl.50159, 2013. 5971

Davin, E. L. and de Noblet-Ducoudré: Climatic impact of global-scale deforestation: radiative versus nonradiative processes, J. Climate, 23, 97–112, doi:10.1175/2009JCLI3102.1, 2010. 5971

Ek, M. B., Mitchell, K. E., Lin, Y., Rogers, E., Grunmann, P., Koren, V., Gayno, G., and Tarpley, J. D.: Implementation of NOAH land surface model advances in the National Centers for Environmental Prediction operational mesoscale Eta model, J. Geophys. Res., 108, 8851, doi:10.1029/2002JD003296, 2003. 5972

Hill, T. C., Williams, M., and Moncrieff, J. B.: Modeling feedbacks between a boreal forest and the planetary boundary layer, J. Geophys. Res., 113, D15122, doi:10.1029/2007JD009412, 2008. 5981

IPCC: Climate Change 2013: The Physical Science Basis. Contribution of Working Group I to the Fifth Assessment Report of the Intergovernmental Panel on Climate Change, Cambridge University Press, Cambridge, UK and New York, NY, USA, 2013. 5971

Jarvis, P. G.: The interpretation of the variations in leaf water potential and stomatal conductance found in canopies in the field, Philos. Trans. Roy. Soc. Lond. B, 273, 593–610, 1976. 5975

Mahrt, L.: Surface heterogeneity and vertical structure of the boundary layer, Bound.-Lay. Meteorol., 96, 33–62, 2000. 5984

Miralles, D. G., van den Berg, M. J., Teuling, A. J., and de Jeu, R. A. M.: Soil moisture-temperature coupling: a multiscale observational analysis, Geophys. Res. Lett., 39, L21707, doi:10.1029/2012GL053703, 2012. 5971

Monteith, J. L.: Evaporation and environment, Symp. Soc. Exp. Biol., XIX, 1965. 5974

Noilhan, J. and Mahfouf, J.-F.: The ISBA land surface parameterisation scheme, Glob. Planet. Change, 13, 145–159, 1996. 5972, 5974

Oren, R., Sperry, J. S., Katul, G. G., Pataki, D. E., Ewers, B. E., Phillips, N., and Schäfer, K. V. R.: Survey and synthesis of intra- and interspecific variation in stomatal sensitivity to vapour pressure deficit, Plant Cell Environ., 22, 1515–1526, 1999. 5973, 5974

Paulson, C. A.: The mathematical representation of wind speed and temperature profiles in the unstable atmospheric surface layer, J. Appl. Meteorol., 9, 857–861, 1970. 5975

Raupach, M. R.: Equilibrium evaporation and the convective boundary layer, Bound.-Lay. Meteorol., 96, 107–141, 2000. 5973

Raupach, M. R.: Combination theory and equilibrium evaporation, Q. J. R. Meteor. Soc., 127, 1149–1181, 2001. 5973

Stap, L. B., van den Hurk, B. J. J. M., van Heerwaarden, C. C., and Neggers, R. A. J.: Modelled contrast in the response of the surface energy balance to heatwaves for forest and grassland, J. Hydrometeorol., doi:10.1175/JHM-D-13-029.1, 2014. 5971

Tennekes, H.: A model for the dynamics of the inversion above a convective boundary layer, J. Atmos. Sci., 30, 558–567, 1973. 5974

Teuling, A. J., Seneviratne, S. I., Stöckli, R., Reichstein, M., Moors, E., Ciais, P., Luyssaert, S., van den Hurk, B., Ammann, C., Bernhofer, C., Dellwik, E., Gianelle11, D., Gielen, B., Grünwald, T., Klumpp, K., Montagnani, L., Moureaux, C., Sottocornola, M., and Wohlfahrt, G.: Contrasting response of European forest and grassland energy exchange to heatwaves, Nat. Geosci., doi:10.1038/NGEO950, 2010. 5970, 5971, 5982

van Heerwaarden, C. C., Vilà-Guerau de Arellano, J., Moene, A. F., and Holtslag, A. A. M.: Interactions between dry-air entrainment, surface evaporation and convective boundary layer development, Q. J. R. Meteor. Soc., 135, 1277–1291, doi:10.1002/qj.431, 2009. 5973, 5991

van Heerwaarden, C. C., Vilà-Guerau de Arellano, J., Gounou, A., Guichard, F., and Couvreux, F.: Understanding the daily cycle of evapotranspiration: a method to quan-

**Forest and grassland energy exchange**

C. C. van Heerwaarden and A. J. Teuling

Title Page

Abstract | Introduction

Conclusions | References

Tables | Figures

◄ | ►

◄ | ►

Back | Close

Full Screen / Esc

Printer-friendly Version

Interactive Discussion

tify the influence of forcings and feedbacks, J. Hydrometeorol., 11, 1405–1422, doi:10.1175/2010JHM1272.1, 2010a. 5972, 5974, 5975, 5982

van Heerwaarden, C. C., Vilà-Guerau de Arellano, J., and Teuling, A. J.: Land-atmosphere coupling explains the link between pan evaporation and actual evapotranspiration trends in a changing climate, Geophys. Res. Lett., 37, L21401, doi:10.1029/2010GL045374, 2010b. 5972, 5976

Vilà-Guerau de Arellano, J., van Heerwaarden, C. C., and Lelieveld, J.: Modelled suppression of boundary-layer clouds by plants in a CO2-rich atmosphere, Nat. Geosci., 5, 701–704, doi:10.1038/NGEO1554, 2012. 5972

Zaitchik, B. F., Macalady, A. K., Bonneau, L. R., and Smith, R. B.: Europe's 2003 heat wave: A satellite view of impacts and land–atmosphere feedbacks., Int. J. Climatol., 26, 743–769, 2006. 5971

Title Page

Abstract | Introduction

Conclusions | References

Tables | Figures

|◀ | ▶|

◀ | ▶

Back | Close

Full Screen / Esc

Printer-friendly Version

Interactive Discussion

**Table 1.** Model parameters specific for forest and grassland. Values taken from the ECMWF IFS documentation (Cy36r1, Table 8.1) using the mixed crops as the value for grassland and the broadleaf deciduous forest for forest.

| variable | description and units | grassland | forest |
|---|---|---|---|
| $\alpha$ | surface albedo [–] | 0.21 | 0.13 |
| $z_{0m}$ | roughness length for momentum [m] | 0.15 | 2.0 |
| $z_{0h}$ | roughness length for heat and moisture [m] | 0.015 | 2.0 |
| $r_{s,\,min}$/LAI | minimum resistance/leaf area index [$s\,m^{-1}$] | 180.0/3.0 | 175.0/5.0 |
| $g_D$ | exponent for VPD response [–] | 0.0 | 0.03 |

**Table A1.** Initial and boundary conditions for all model runs.

| Variable | Description and unit | Values |
|---|---|---|
| $P_0$ | surface pressure [Pa] | 101300.0 |
| lat | latitude [deg] | $50°$ N |
| lon | longitude [deg] | $0°$ E |
| doy | day of the year [–] | 182.0 |
| $t_{start}$ | start time of simulation in local time [h] | 7 |
| $t_{end}$ | end time of simulation in local time [h] | 17 |
| cc | cloud cover [–] | $cc_{input}$ |
| $w_g$ | volumetric water content top soil layer [$m^3 m^{-3}$] | 0.235 |
| $w_2$ | volumetric water content deeper soil layer [$m^3 m^{-3}$] | 0.235 |
| $c_{veg}$ | vegetation fraction [–] | 0.9 |
| $T_{soil}$ | temperature top soil layer [K] | $T_{input} - 3$ |
| $T_2$ | temperature deeper soil layer [K] | $T_{input} - 2$ |
| $a$ | Clapp and Hornberger retention curve parameter [–] | 0.219 |
| $b$ | Clapp and Hornberger retention curve parameter [–] | 4.90 |
| $p$ | Clapp and Hornberger retention curve parameter [–] | 4.0 |
| $CG_{sat}$ | saturated soil conductivity for heat [$K m^{-2} J^{-1}$] | $3.56 \times 10^{-6}$ |
| $w_{sat}$ | saturated volumetric water content [$m^3 m^{-3}$] | 0.472 |
| $w_{fc}$ | volumetric water content field capacity [$m^3 m^{-3}$] | 0.323 |
| $w_{wilt}$ | volumetric water content wilting point [$m^3 m^{-3}$] | 0.171 |
| $C1_{sat}$ | Coefficient force term moisture [–] | 0.132 |
| $C2_{ref}$ | Coefficient restore term moisture [–] | 1.8 |
| LAI | leaf area index [–] | see Table 1 |
| $r_{s, min}$ | minimum resistance transpiration [$s m^{-1}$] | |
| $z_{0m}$ | roughness length for momentum [m] | |
| $z_{0h}$ | roughness length for heat and moisture [m] | |
| $\alpha$ | surface albedo [–] | |
| $g_D$ | exponent for VPD response | |
| $h$ | initial ABL height [m] | 200.0 |
| $\theta$ | initial mixed layer potential temperature [K] | $T_{input}$ |
| $d\theta$ | initial temperature jump at $h$ [K] | $T_{input} + 5$ |
| $\gamma_\theta$ | free atmosphere potential temperature lapse rate [$K m^{-1}$] | 0.006 |
| $A_{\theta_v}$ | entrainment ratio for virtual potential temperature [–] | 0.2 |
| $q$ | initial mixed layer specific humidity [$kg kg^{-1}$] | RH = 0.7 |
| $dq$ | initial specific humidity jump at $h$ [$kg kg^{-1}$] | −0.002 |
| $u$ | initial mixed layer wind speed [$m s^{-1}$] | 7.0 |
| ug | geostrophic wind speed [$m s^{-1}$] | 10.0 |

Title Page

Abstract | Introduction

Conclusions | References

Tables | Figures

◄ | ►

◄ | ►

Back | Close

Full Screen / Esc

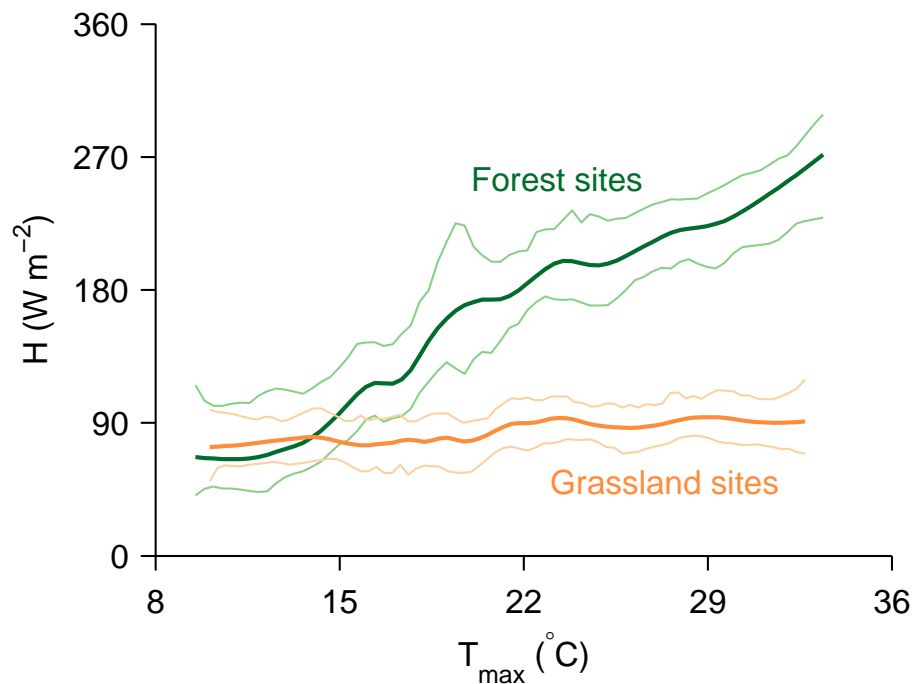Printer-friendly Version

Interactive Discussion

**Fig. 1.** Observed midday sensible heat fluxes ($H$) over forest and grassland sites as a function of daily maximum air temperature. Curves have been derived using locally weighted polynomial regression (LOESS) on all midday data (09:00–13:00 UTC), heat wave days included, in the months June–August for all European FLUXNET sites analysed in T10. Uncertainty bounds reflect 5% and 95% percentiles of the LOESS regression as determined by bootstrapping. See Supplement in T10 for more information.

Full Screen / Esc

Printer-friendly Version

Interactive Discussion
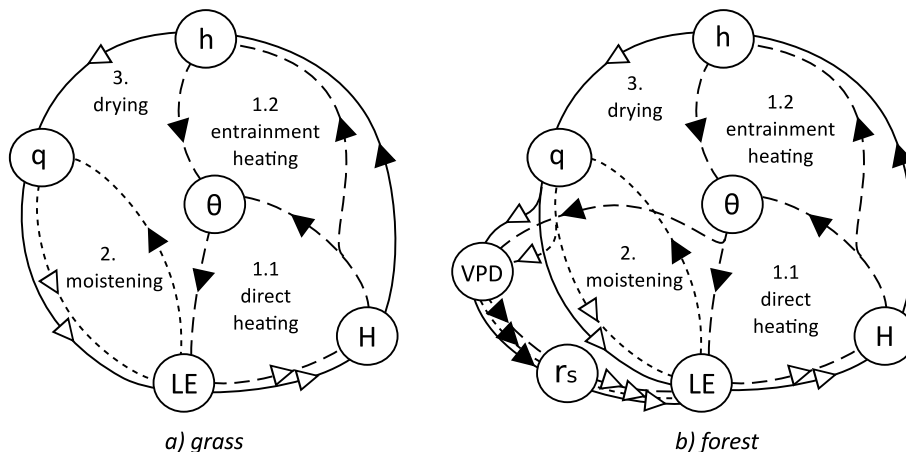
**Fig. 2.** Overview of the most relevant feedback loops between the land surface and the atmospheric boundary layer for forest and grassland (left figure comes from van Heerwaarden et al., 2009). Closed triangles show positive correlations, open triangles negative ones. Each linestyle describes a distinct feedback loop. LE is the evapotranspiration, $H$ is the sensible heat flux, $\theta$ and $q$ are the potential temperature and the specific humidity of the convective boundary layer, $h$ is the height of that layer, VPD is the vapor pressure deficit at the vegetation level and $r_s$ is the stomatal resistance.

Full Screen / Esc

Printer-friendly Version

Interactive Discussion
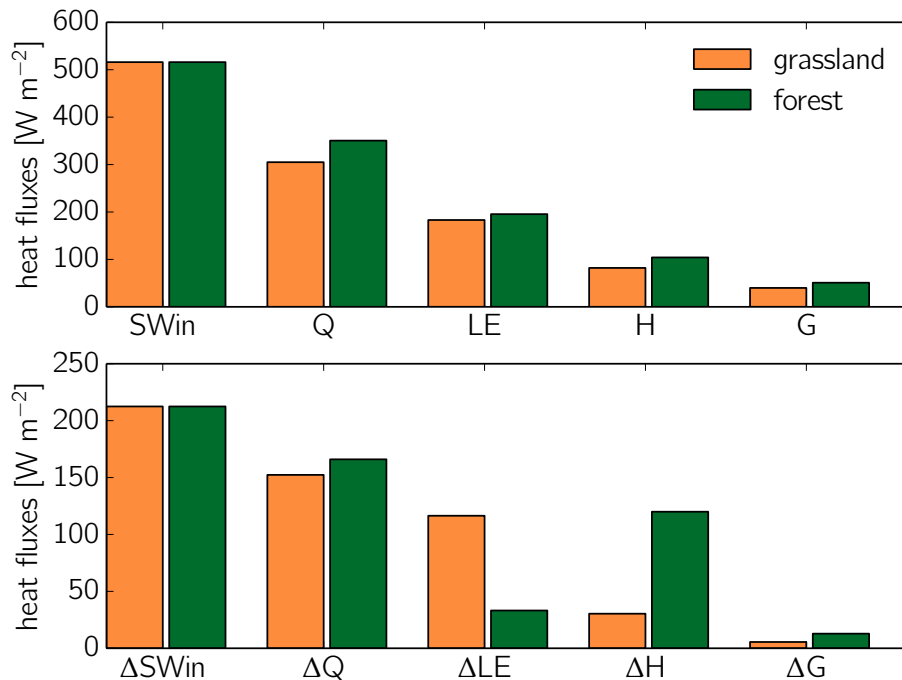


**Fig. 3.** The surface energy balance under standard conditions (top panel) and under heat wave conditions (bottom panel) as computed in the modeling experiment. The values are the 10 h means over the entire duration of the model run. The difference is computed by subtracting the mean state from the heat wave conditions.
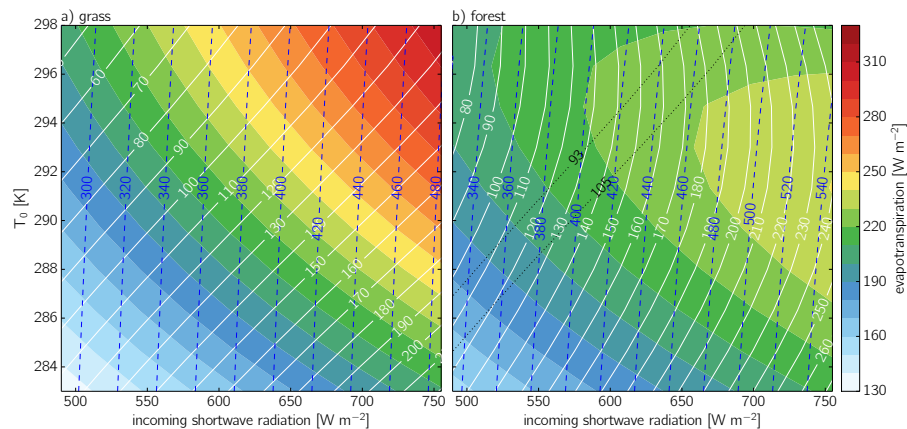
**Fig. 4.** Evapotranspiration or latent heat flux (shades), sensible heat flux (white solid lines) and net radiation (blue dashed lines). The values are the 10 h means over the entire duration of the model run. The black dotted lines correspond to the range in which grassland gives a constant sensible heat flux with similar magnitudes as those in the observations in Fig. 1.

Title Page

Abstract          Introduction

Conclusions          References

Tables          Figures

I◄          ►I

◄          ►

Back          Close

Full Screen / Esc

Printer-friendly Version

Interactive Discussion
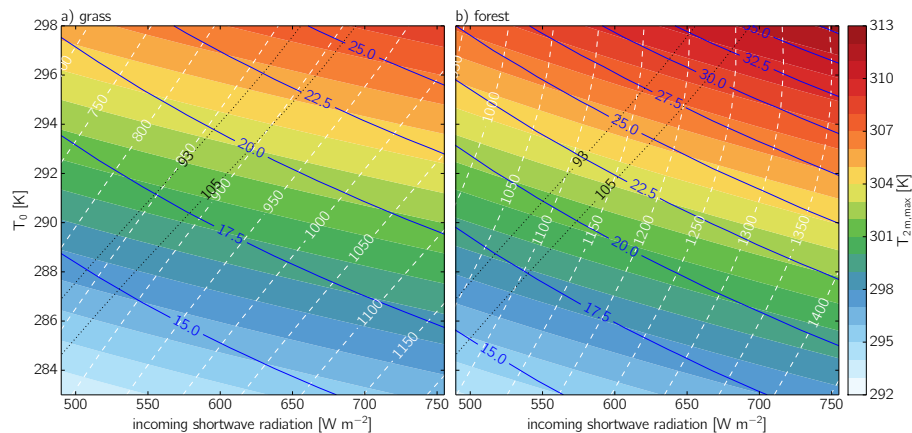
**Fig. 5.** Maximum temperatures (shades), vapor pressure deficit (blue solid lines) and boundary layer height (white dashed lines). The values for the VPD (hPa) and the boundary layer height (m) are the 10 h means over the entire duration of the model run, the maximum 2 m temperature is the maximum over the duration. The black dotted lines correspond to the range in which grassland gives a constant sensible heat flux with similar magnitudes as those in the observations in Fig. 1.
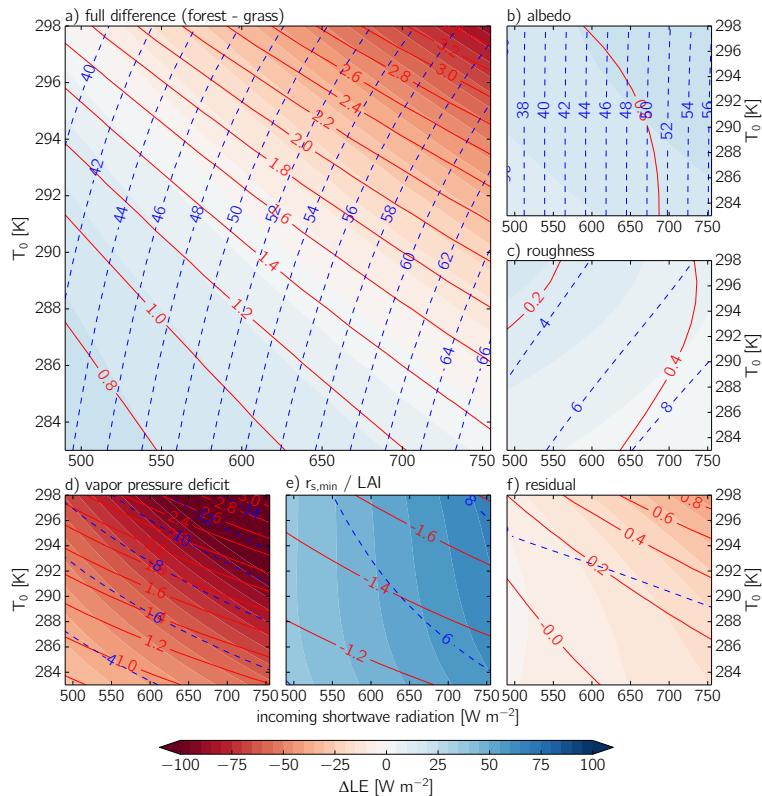
**Fig. 6.** Difference in evapotranspiration (shades), maximum temperature (red solid line) and net radiation (blue dashed line) between forest and grassland as a function of initial temperature and incoming shortwave radiation. Small panels indicate the contribution of individual processes/parameters, such that the values in the small panels sum up to the value in the large panel. The values for evapotranspiration and net radiation are the 10 h means over the entire duration of the model run, the maximum 2 m temperature is the maximum over the entire duration.

Title Page

Abstract | Introduction

Conclusions | References

Tables | Figures

|◄ | ►|

◄ | ►

Back | Close

Full Screen / Esc

Printer-friendly Version

Interactive Discussion